

INFLUENCE OF MANUFACTURING METHOD AND SURFACE CONDITION
ON THE FATIGUE STRENGTH OF Ti-6Al-4V MATERIAL

J. Broichhausen, M. Telfah

Rhein.-Westf. Techn. Hochschule, Aachen

Highly stressed Ti-6Al-4V parts must have high-quality surfaces to ensure maximum fatigue strength. As a general rule, however, such parts have to be machined because their surface finish is inadequate. Under these circumstances the basic requirement is as follows:

Manufacture of close-to-form mill products having a high-quality surface finish. Normally the surface requirement will not be met, and therefore it was decided to investigate whether the actual finish of these products can be sufficiently improved by suitable surface treatments.

This investigation is based on the fatigue strengths obtained on test specimens manufactured by the following methods permitting the production of close-to-form shapes:

Die forging
Hot isostatic pressing (powder metallurgy)
Precision casting.

The test specimens used had a rectangular cross-section of 4 mm x 16 mm. For comparison, the investigation also included specimens that had been machined all over and then polished over their entire gauge length in the axial direction (surface roughness $\leq 0.5 \mu\text{m}$).

The die-forged test specimens notches in the flashline area due to the trimming operation. These notches, which can be avoided, have a detrimental effect on actual fatigue strength, and with the exception of one test series the narrow sides of the specimens were therefore machined prior to any subsequent surface treatment. These specimens were subjected to the standard processes indicated in Fig. 1.

The metal powder used for the HIP parts was produced at CENG (Centre d'Etude Nationale Grenoble) in France by electron-beam melting, the grit size ranging from 640 to 40 μm diameter. The tubular containers (80 mm diameter, 200 mm length) were made from unalloyed steel.

After heating the vacuum-tight welded containers in a vacuum, the Ti-6Al-4V powder was filled into the pre-evacuated containers by means of a vacuum filling plant. Following degassing of the powder at 450°C and continuous evacuation for 16 hours, the filler neck was welded vacuum-tight. The actual HIP operation was performed at a pressure of 1500 bar and a temperature of 920°C for 3 hours.

The precision cast specimens were tested either complete with scale or with their surfaces machined all over.

The alternating tension-compression fatigue strength of the test material was determined by single-stage testing at an ultimate number of cycles of 2×10^7 . Fig. 1 summarises the various investigations and also the results obtained.

A critical evaluation of these data results in the following

conclusions:

- High-strength parts cannot be manufactured by precision casting because their fatigue strength is too low.
- The results of shot peening did not come up to expectations. Partly this is due to the rectangular cross-section of the test specimens, but even more so to their inadequate surface finish.
- The test specimens taken from Ti-6Al-4V HIP parts did not give the fatigue strength values that were to be expected.

A comparison between the actual surface finishes and the relevant fatigue strength (Fig. 2) reveals direct interdependence.

Due to the fact that the HIP test specimens did not have the expected fatigue strength level, further tests were carried out in order to establish the reasons for the disappointing fatigue behaviour of this material.

As only 12 standard test specimens could be taken from the available HIP material, additional sub-standard specimens of 2 mm gauge diameter were machined from the grip heads of used standard specimens for further investigations regarding the level and directionality of alternating tension-compression strengths. The results of these tests are presented in Fig. 3.

This diagram shows that the results obtained on both standard and sub-standard test specimens scatter widely, and that actual fatigue strength is inadequate

The material has a plate-like, equiaxed structure, and most of the alpha plates are arranged in groups (Fig. 4). There are numerous inhomogeneous spherical spots which show up on the microphotos as annular surfaces with an enclosed core (Fig. 5). In these areas the actual hardness is higher than that of the matrix (Fig. 6). The difference in hardness ranges from 35 to 100 Vickers units, indicating an embrittled condition of such areas.

When the distribution of concentrations in the area shown in Fig. 7a was examined, aluminium enrichment and a lower vanadium concentration were found in the annular surface compared with the matrix (Fig. 7b).

The fracture surfaces indicate that fatigue cracks tended to originate in such areas (Fig. 8). It was found that the concentration of aluminum at the fatigue origin was also higher than that of the surrounding material (Fig. 9).

In the area of fatigue fracture one also found spherical inclusions which appear to be identical with the above-mentioned inhomogeneous spots because these areas show an aluminium enrichment compared with the matrix (Fig. 10).

A transverse section through the fatigue origin confirmed that the inhomogeneous areas are preferred fracture origins and therefore have a considerable influence on actual fatigue strength (Fig. 11). At such locations an intercrystalline weakness of the structure was found to exist.

The results of a structural analysis in an inhomogeneous area by

means of transmission and diffraction photos from thin microsections with a 5 % tolerance in respect of the appropriate ASTM cards were as follows:

In the annular surface the alpha phase showed alpha₂ segregations (Fig. 12). These have a hexagonal superstructure and are the result of the existing aluminium enrichment. The higher hardness values found in such areas are due to these segregations.

The core surrounded by the annular surface does not significantly differ from the matrix. Only at the fringe a few alpha₂ segregations were traceable as reflexes.

The diffraction patterns did not permit to define the segregations clearly, but it was estimated that these are alpha₂ segregations with the following lattice parameters: $a_0 = 5.77$ and $c_0 = 4.62$ as well as $a_0 = 11.52$ and $c_0 = 4.65$.

The results of the investigations covered by this paper can be summarised as follows:

- Under the circumstances the surface treatments examined did not sufficiently improve the fatigue strength of die-forged test specimens.
- The HIP test specimens were found to contain defects reducing their fatigue strength significantly. These defects can be avoided, however, and defect-free specimens are expected to have a considerably higher fatigue strength.

References

1. J. Broichhausen, H. van Kann: Joint Conference, Leeds 1977
2. J. Broichhausen, M. Telfah: Forschungsbericht des Landes Nordrhein-Westfalen No. 2853

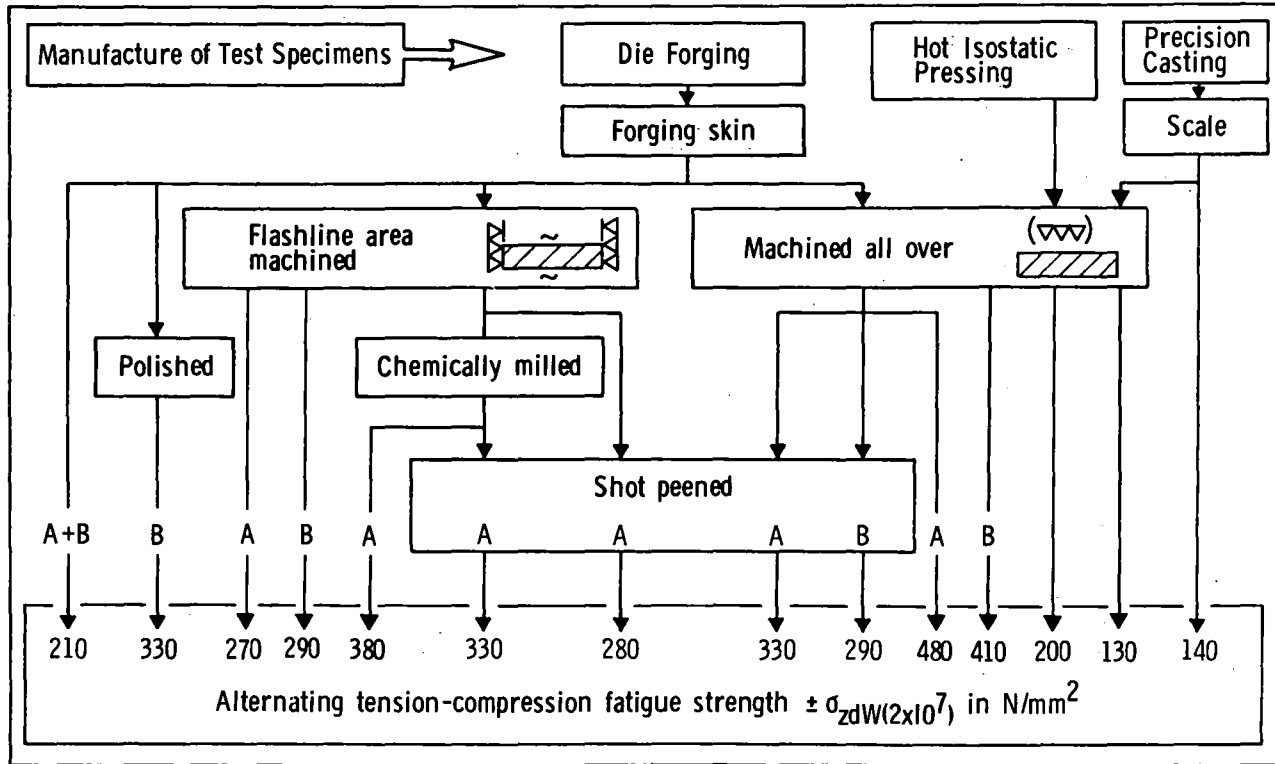


Fig. 1: Manufacture of Test Specimens; Surface Conditions and Treatments; Fatigue Strength

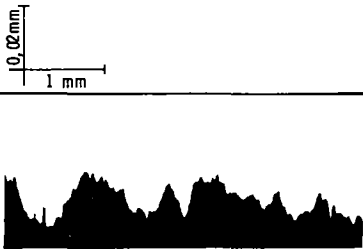
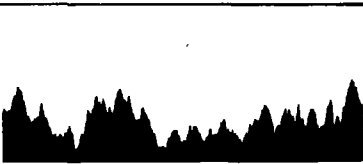




Surface Condition	Lot No.				Surface Finish
	$\pm\sigma_{zdW}$ N/mm ²	A β_k^*	$\pm\sigma_{zdW}$ N/mm ²	B β_k^*	
Forging skin of test specimens machined	210	2,30	210	1,95	
	270	1,80	290	1,41	
	280	1,71	-	-	
	190	2,40	-	-	
	380	1,26	-	-	
	330	1,45	-	-	
	-	-	330	1,24	
	Machined all over	-	-	290	1,41
480		1,00	410	1,00	
330		1,45	-	-	

Fig.2: Comparison of Fatigue Strength and Surface Roughness

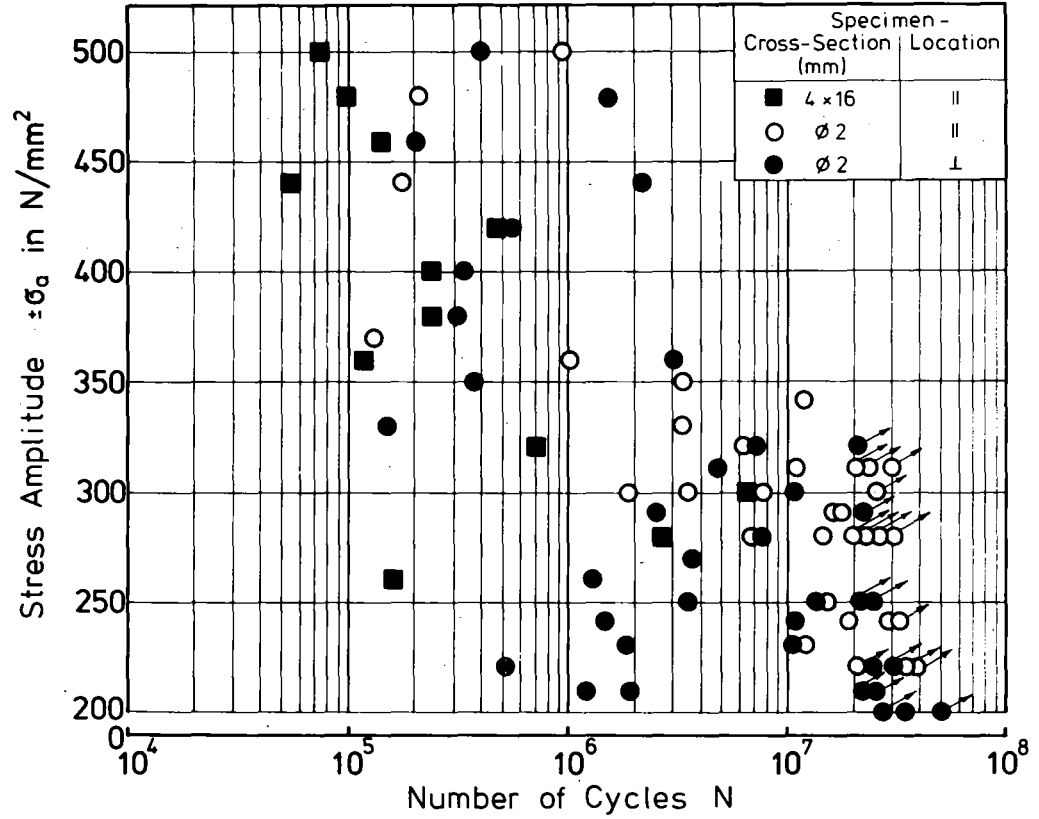


Fig. 3: Fatigue Strength of P/M HIP Test Specimens

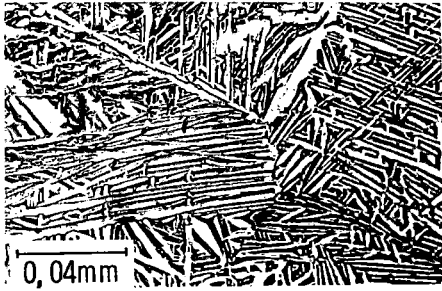
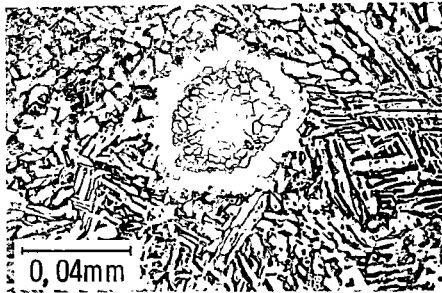


Fig. 4: Structure



Axial direction



Transverse direction

Fig. 5: Structural Defects

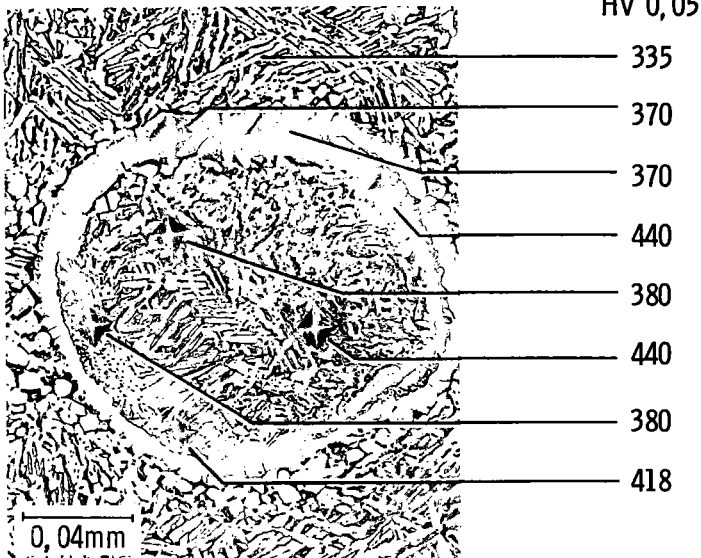


Fig. 6: Distribution of Micro Hardness over an Inhomogeneous Area of the Structure

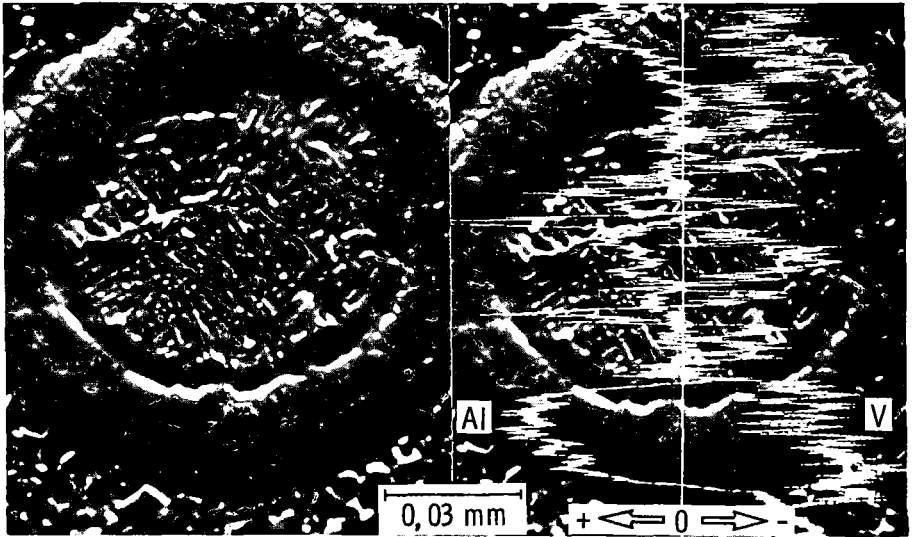


Fig 7: Distribution of Aluminium und Vanadium Concentrations

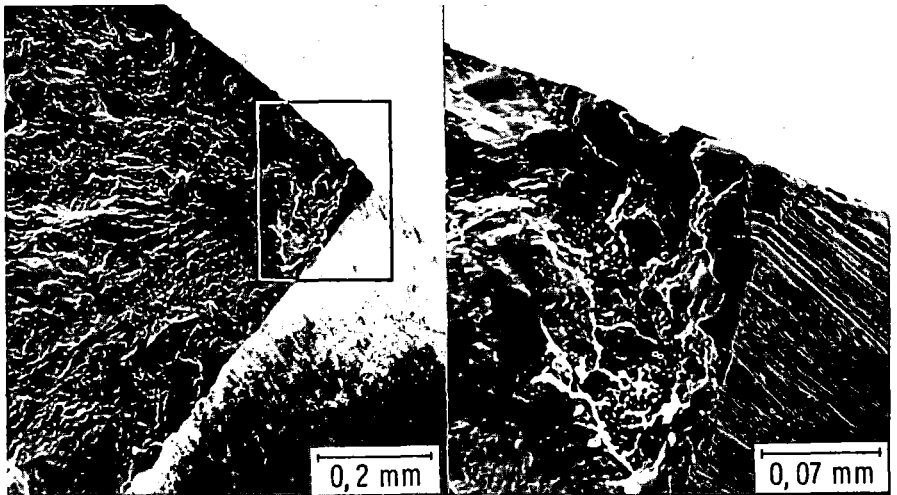


Fig 8: Fatigue Origin

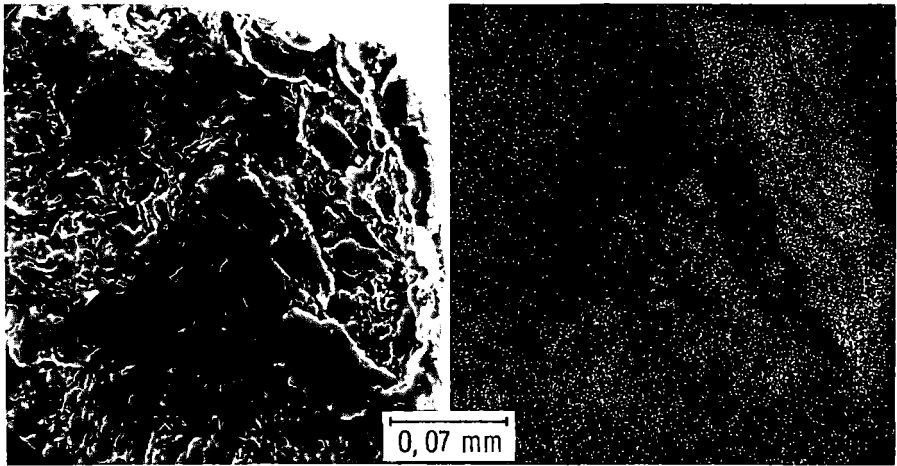


Fig. 9: Distribution of Aluminium at Fatigue Origin

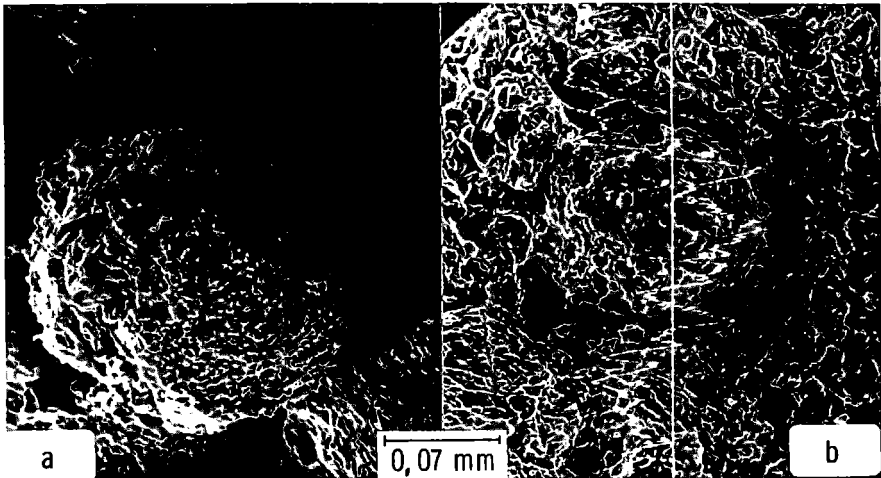


Fig. 10: Spherical Inclusions in the Fatigue Fracture Surface
a) Crack Formation
b) Distribution of Aluminium

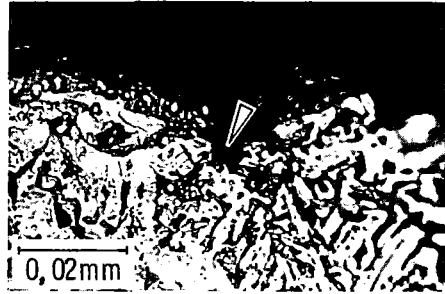


Fig. 11: Fatigue Origin

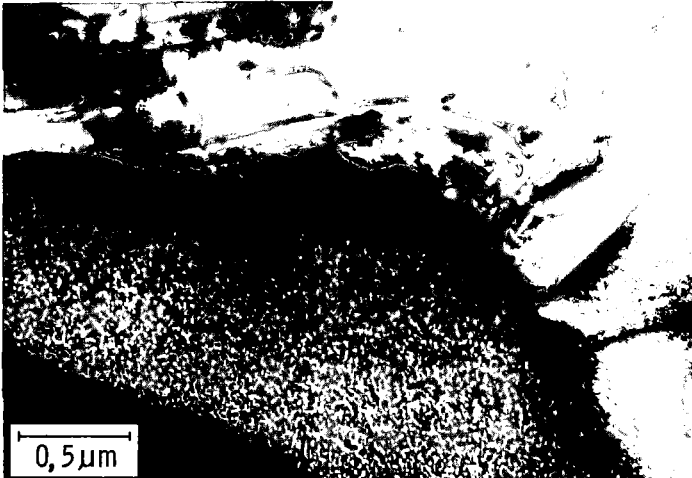


Fig. 12: Seregations in the Structure of the Annular Surface